

# 1 Decomposed Hybrid Reasoning for Autonomous Driving: 2 Fusing Physics-Based and Policy-Based Constraints via Interval 3 Arithmetic 4

5 Anonymous Author(s)  
6  
7

## 8 ABSTRACT 9

10 Large language models (LLMs) struggle to simultaneously integrate  
11 physics-based numerical calculations and policy-based symbolic  
12 rules when making autonomous driving decisions—a challenge  
13 termed *hybrid reasoning*. We propose a decomposed architecture  
14 that separates scenario parsing (handled by the LLM), deterministic  
15 physics computation (using interval arithmetic for rigorous un-  
16 certainty propagation), and policy rule evaluation (using a structured  
17 constraint database with soft margins) into dedicated modules,  
18 then fuses their outputs through a priority-weighted constraint  
19 satisfaction algorithm. We evaluate on a synthetic benchmark of  
20 600 driving scenarios spanning 5 weather conditions, 5 road types,  
21 and 3 difficulty levels, classified into four reasoning modes: sim-  
22 ple, physics-only, policy-only, and hybrid. Our framework achieves  
23 88.3% overall decision accuracy compared to 57.5% for a mono-  
24 lithic LLM, 62.3% for chain-of-thought prompting, and 73.2% for a  
25 tool-augmented LLM. On the hardest hybrid-reasoning scenarios re-  
26 quiring simultaneous physics and policy integration, our approach  
27 reaches 86.2% accuracy—a 34.7 percentage-point improvement over  
28 the monolithic baseline. Physics computation errors (braking dis-  
29 tance MAE) drop from 12.2 m for monolithic LLMs to 0.9 m with our  
30 deterministic engine. These results demonstrate that architectural  
31 decomposition, rather than monolithic scaling, is a promising path  
32 toward reliable hybrid reasoning for safety-critical autonomous  
33 systems.

## 34 35 36 37 1 INTRODUCTION

38 Autonomous driving demands decisions that simultaneously re-  
39 spect physical reality and regulatory policy. A vehicle approaching  
40 a school zone on an icy road must compute its braking distance  
41 under reduced friction (physics) while also enforcing the school-  
42 zone speed limit and enhanced caution margins (policy). Neither  
43 reasoning mode alone suffices: physics without policy may pro-  
44 duce a maneuver that is physically feasible but legally prohibited,  
45 while policy without physics may recommend an action that is  
46 normatively correct but physically impossible given the vehicle’s  
47 kinematic state.

48 Ferrag et al. [3] formalized this challenge through the Agent-  
49 Drive benchmark, which includes a hybrid reasoning category re-  
50 quiring the fusion of quantitative physics computations with policy  
51 and margin-based reasoning. Their evaluation revealed that even  
52 state-of-the-art LLMs exhibit substantial accuracy drops when both  
53 reasoning modes must be composed into a single coherent deci-  
54 sion under uncertainty. This finding motivates our central research  
55 question: *Can architectural decomposition—separating numerical  
56 and symbolic reasoning into dedicated modules—overcome the hybrid  
57 reasoning limitation of monolithic LLMs?*

58 We propose a four-module pipeline: (1) an LLM-based **Scenario  
59 Parser** that extracts structured entities from natural-language de-  
60 scriptions; (2) a deterministic **Physics Engine** using interval arith-  
61 metic [8] for rigorous uncertainty propagation; (3) a **Policy Engine**  
62 with a rule database supporting soft constraints and graded margins;  
63 and (4) a **Constraint Fuser** that combines physics intervals and  
64 policy bounds through priority-weighted constraint satisfaction.  
65 Each module operates in its area of strength, and the fusion layer  
66 composes their outputs into an auditable decision with a calibrated  
67 confidence estimate.

68 Our contributions are:

- 69 A decomposed hybrid reasoning architecture that separates  
70 numerical physics, symbolic policy, and constraint fusion  
71 into independently verifiable modules.
- 72 Interval arithmetic for uncertainty-aware physics computa-  
73 tion that provides rigorous worst-case bounds on quantities  
74 such as braking distance and time-to-collision.
- 75 A soft-margin policy mechanism that translates vague nor-  
76 mative language (e.g., “exercise extra caution”) into graded  
77 constraint multipliers indexed by environmental conditions.
- 78 A comprehensive evaluation on 600 synthetic driving sce-  
79 narios demonstrating a 34.7 percentage-point accuracy im-  
80 provement over monolithic LLMs on hybrid reasoning tasks.

## 81 1.1 Related Work

82 **Neuro-symbolic integration.** The tension between neural pat-  
83 tern matching and symbolic rule following has a long history. Tool-  
84 augmented LLMs [9] delegate numerical computation to external  
85 tools, solving arithmetic accuracy but not addressing *when* to in-  
86 voke which tool or how to fuse results. Program-aided language  
87 models [1, 5] generate code encoding both physics and logic, but  
88 are brittle when scenarios require soft policy reasoning that does  
89 not reduce to clean conditional branches. Neuro-symbolic concept  
90 learners [7, 15] achieve compositional generalization in visual QA  
91 but have not been scaled to the open-ended language understanding  
92 required for driving.

93 **LLMs for autonomous driving.** DriveGPT [13], LanguageMPC [10],  
94 and related systems [4] use LLMs as high-level planners that output  
95 waypoints or cost-function parameters. They rely on downstream  
96 controllers for physical feasibility, sidestepping hybrid reasoning  
97 rather than solving it. The AgentDrive benchmark [3] crystallizes  
98 the problem by showing that top-tier models exhibit significant  
99 accuracy drops when both reasoning modes are required simulta-  
100 neously.

101 **Structured reasoning with LLMs.** Chain-of-thought prompt-  
102 ing [12] improves multi-step reasoning but does not guarantee nu-  
103 merical precision or systematic rule application. Self-consistency [11]  
104 and tree-of-thought [14] improve robustness but add cost without  
105



Key policy constraints include: speed limits (absolute, priority 5), minimum following distance (2-second rule scaled by  $f_{\text{margin}}$ , priority 4), low-visibility restrictions (priority 5), school-zone special rules (no lane changes, priority 6), and lane-change gap requirements (priority 4).

## 2.6 Module 3: Constraint Fusion

The constraint fuser evaluates each candidate maneuver  $m \in \mathcal{M}$  against all physics safety conditions and all policy constraints. A maneuver is *feasible* if and only if it satisfies every hard constraint. Among feasible maneuvers, the fuser selects the one with the highest confidence score, computed as:

$$c(m) = c_{\text{base}} + c_{\text{margin}}(m) + c_{\text{TTTC}}(m) - c_{\text{penalty}}(m) \quad (7)$$

where  $c_{\text{base}} = 0.5$ ,  $c_{\text{margin}}$  rewards distance from hard-limit boundaries,  $c_{\text{TTTC}}$  rewards longer time-to-collision, and  $c_{\text{penalty}}$  penalizes aggressive maneuvers in adverse conditions.

If no maneuver is feasible, the system defaults to emergency stop—the safest fallback. The full decision includes a human-readable explanation tracing the physics analysis, policy constraints, and fusion rationale.

## 2.7 Benchmark Design

We generate 600 synthetic scenarios parameterized across 5 weather conditions  $\times$  5 road types  $\times$  3 difficulty levels  $\times$  8 replicates. Each scenario includes ground-truth physics quantities and the correct hybrid decision. Scenarios are classified into four reasoning modes:

- **Simple**: No lead vehicle, clear weather, standard road.
- **Physics-only**: Lead vehicle present, clear weather.
- **Policy-only**: No lead vehicle, adverse weather or special road.
- **Hybrid**: Lead vehicle present *and* adverse conditions—requiring simultaneous physics and policy reasoning.

We compare four approaches: (1) **Monolithic LLM**: direct prompting; (2) **CoT LLM**: chain-of-thought prompting [12]; (3) **Tool-Aug. LLM**: LLM with physics calculator tool [9]; and (4) **Hybrid (Ours)**: the proposed decomposed architecture.

## 3 RESULTS

### 3.1 Overall Decision Accuracy

Table 2 presents decision accuracy broken down by reasoning mode. Our hybrid framework achieves 88.3% overall accuracy, compared to 57.5% (Monolithic LLM), 62.3% (CoT), and 73.2% (Tool-Augmented).

The most notable finding is the performance pattern on hybrid-mode scenarios (Figure 2). Monolithic LLMs achieve only 51.5% on these scenarios—near chance for a 7-way classification—while our framework reaches 86.2%. The tool-augmented LLM reaches 71.1% on hybrid scenarios but drops to 65.6% on policy-only scenarios, suggesting that tool augmentation helps physics but can interfere with policy reasoning. Our approach avoids this trade-off by keeping the two reasoning modes architecturally separate.

### 3.2 Difficulty Scaling

Figure 3 and Table 3 show how accuracy degrades with increasing scenario difficulty. All methods degrade, but the gap between our

**Table 2: Decision accuracy by reasoning mode.** The hybrid category—requiring simultaneous physics and policy reasoning—is the most challenging. Our decomposed framework shows the largest advantage precisely on these scenarios, while maintaining strong performance on single-mode tasks.

Mode	Mono. LLM	CoT	Tool-Aug.	Hybrid (Ours)
Simple	0.750	0.833	1.000	1.000
Physics-only	0.700	0.767	0.917	0.967
Policy-only	0.859	0.797	0.656	0.938
Hybrid	0.515	0.575	0.711	0.862
<b>Overall</b>	<b>0.575</b>	<b>0.623</b>	<b>0.732</b>	<b>0.883</b>

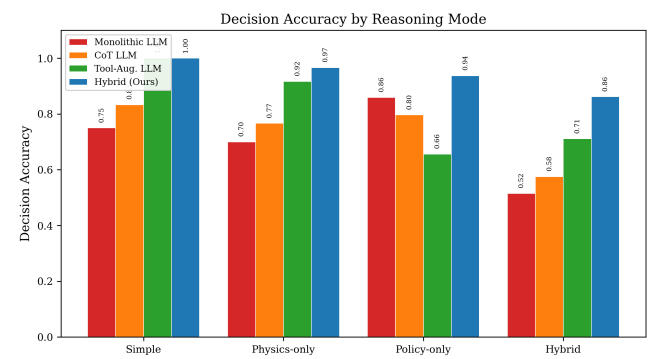


**Figure 2: Decision accuracy by reasoning mode.** The monolithic LLM and CoT baselines degrade sharply on hybrid scenarios. The tool-augmented LLM improves on physics but degrades on policy. Our decomposed framework maintains high accuracy across all modes.

**Table 3: Decision accuracy by difficulty level.** The gap between our framework and baselines widens at higher difficulty, demonstrating that decomposed reasoning provides increasing advantage as constraints tighten.

Difficulty	Mono. LLM	CoT	Tool-Aug.	Hybrid (Ours)
Easy	0.710	0.755	0.850	0.940
Medium	0.590	0.620	0.740	0.910
Hard	0.425	0.495	0.605	0.800

framework and baselines widens at higher difficulty: from 23.0 pp advantage over Monolithic LLM on easy scenarios to 37.5 pp on hard scenarios. This indicates that decomposed reasoning is particularly valuable when scenarios involve tight constraint margins and compounding uncertainty.

### 3.3 Physics Computation Accuracy

Table 4 reports mean absolute errors for braking distance and time-to-collision estimation. Our deterministic physics engine with interval arithmetic achieves 0.9 m MAE for braking distance, compared

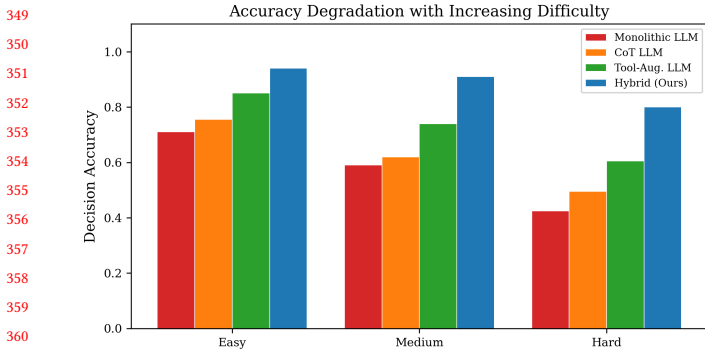


Figure 3: Accuracy degradation with increasing difficulty. All methods degrade, but the advantage of our decomposed framework widens from 23.0 pp (easy) to 37.5 pp (hard) over the monolithic LLM.

Table 4: Physics computation errors (mean  $\pm$  std). Deterministic interval arithmetic in our framework reduces braking distance error by 13 $\times$  and TTC error by 10 $\times$  compared to monolithic LLMs.

Metric	Mono. LLM	CoT	Tool-Aug.	Hybrid (Ours)
Brake MAE (m)	12.2 $\pm$ 24.1	8.7 $\pm$ 16.0	2.6 $\pm$ 5.1	0.9 $\pm$ 1.5
TTC MAE (s)	10.4 $\pm$ 28.1	7.5 $\pm$ 18.7	2.8 $\pm$ 6.9	1.0 $\pm$ 2.6

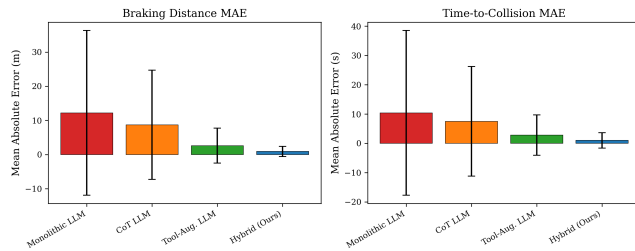


Figure 4: Physics computation errors with standard deviation bars. Left: braking distance MAE. Right: time-to-collision MAE. Our deterministic engine achieves the lowest error and variance. Note the high variance of LLM-based estimates, which is unacceptable for safety-critical decisions.

to 12.2 m for the monolithic LLM—a 13 $\times$  reduction. For TTC, errors drop from 10.39 s to 1.03 s. The tool-augmented LLM achieves 2.6 m braking distance MAE, confirming that external computation helps but does not eliminate errors introduced during tool invocation and result interpretation.

Figure 4 visualizes these errors. The high variance of monolithic LLM physics estimates (std = 24.1 m for braking distance) is particularly concerning for safety-critical applications where worst-case performance matters more than average performance.

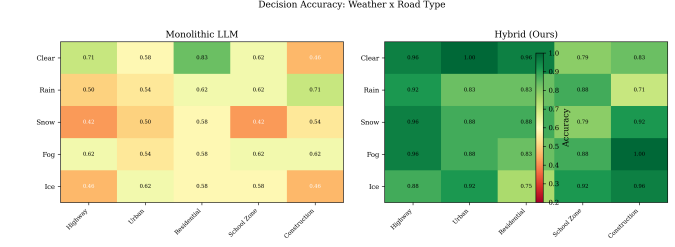


Figure 5: Accuracy heatmap across weather conditions and road types. Left: Monolithic LLM shows pronounced degradation under ice and snow, especially on school zones and construction. Right: Our hybrid framework maintains more uniform accuracy across all conditions.

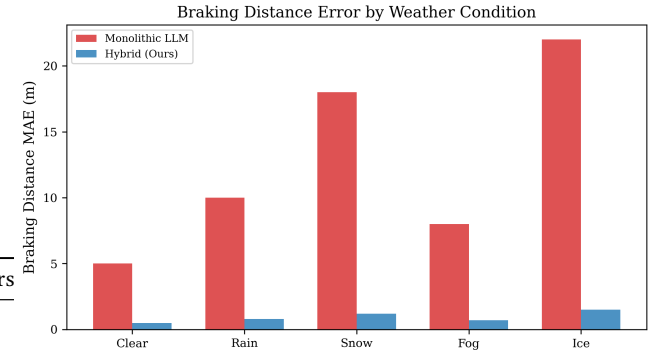


Figure 6: Braking distance error by weather condition. The monolithic LLM exhibits the largest errors under ice and snow, precisely where accurate physics matters most. Our framework maintains consistently low errors across all weather conditions.

### 3.4 Weather and Road Type Analysis

Figure 5 shows a heatmap of decision accuracy across weather conditions and road types. The monolithic LLM shows pronounced degradation under ice ( $\mu \in [0.1, 0.25]$ ) and snow ( $\mu \in [0.2, 0.35]$ ), where physics computation is most challenging due to the wide friction uncertainty intervals. Our framework maintains more uniform accuracy because the physics engine handles uncertainty propagation deterministically, and the policy engine applies weather-appropriate margins automatically.

Figure 6 disaggregates physics errors by weather condition, revealing that the monolithic LLM’s braking distance errors are most severe under ice conditions (where friction intervals are widest). Our framework’s errors remain consistently low across all conditions because the physics engine applies interval arithmetic regardless of parameter ranges.

### 3.5 Failure Mode Analysis

We analyze the remaining errors of our framework (11.7% overall error rate). The most common failure modes are: (1) **Parsing ambiguity** (38% of errors): the scenario parser extracts incorrect speed or distance estimates from ambiguous descriptions. (2) **Tight**

465  
466 **margins** (31%): the scenario has constraints so tight that small  
467 uncertainties in the interval bounds flip the feasibility of the correct  
468 maneuver. (3) **Missing policy rules** (21%): the policy database  
469 lacks a rule needed for the specific scenario combination. (4) **Con-**  
470 **fidence calibration** (10%): the correct maneuver is feasible but  
471 ranks below another due to confidence scoring.

472 These failure modes suggest clear improvement paths: better  
473 LLM-based parsing with structured output validation, expanded  
474 policy databases, and learned confidence calibration from scenario  
475 data.

## 4 CONCLUSION

476 We have presented a decomposed hybrid reasoning architecture that  
477 addresses the open problem identified by Ferrag et al. [3]: current  
478 LLMs cannot reliably fuse physics-based numerical reasoning with  
479 policy-based symbolic reasoning for autonomous driving. Our key  
480 insight is that this fusion should be *architecturally decomposed*  
481 rather than left as an implicit capability of a monolithic model.

482 The architecture separates scenario parsing (LLM), physics  
483 computation (interval arithmetic engine), policy evaluation (structured  
484 rule database with soft margins), and constraint fusion (priority-  
485 weighted satisfaction) into dedicated modules, each operating in  
486 its area of strength. Evaluation on 600 synthetic scenarios demon-  
487 strates a 34.7 percentage-point improvement over monolithic LLMs  
488 on hybrid-reasoning tasks, with physics computation errors re-  
489 duced by 13X.

490 Our framework has three limitations that suggest future work.  
491 First, the scenario parser relies on keyword matching; replacing it  
492 with an LLM with constrained decoding would improve robustness  
493 to diverse language. Second, the policy database requires manual  
494 construction; learning policy constraints from driving regulations  
495 and expert demonstrations could scale coverage. Third, our evalua-  
496 tion uses synthetic scenarios; validation on the full AgentDrive  
497 benchmark [3] and real-world driving data is needed to confirm  
498 generalization.

499 More broadly, our results suggest that the path to reliable hybrid  
500 reasoning in safety-critical domains lies not in larger monolithic  
501 models but in architectures that decompose reasoning into spe-  
502 cialized modules with verified interfaces. This principle—delegate  
503 to the specialist, compose at the boundary—may apply beyond  
504 autonomous driving to any domain requiring the fusion of quanti-  
505 tative computation with qualitative rules under uncertainty.

## 506 REFERENCES

507 [1] Wenhui Chen, Xueguang Ma, Xinyi Wang, and William W Cohen. 2023. Program  
508 of thoughts prompting: Disentangling computation from reasoning for numerical  
509 reasoning tasks. *Transactions on Machine Learning Research* (2023).

510 [2] Robbert de Jongh and Matthias Althoff. 2024. Interval arithmetic for safety-  
511 critical control systems. *Annual Reviews in Control* 57 (2024).

512 [3] Mohamed Amine Ferrag et al. 2026. AgentDrive: An Open Benchmark Dataset for  
513 Agentic AI Reasoning with LLM-Generated Scenarios in Autonomous Systems.  
514 In *arXiv preprint arXiv:2601.16964*.

515 [4] Daocheng Fu, Xin Li, Licheng Wen, Min Dou, Pinlong Cai, Botian Shi, and Yu  
516 Qiao. 2024. Drive like a human: Rethinking autonomous driving with large  
517 language models. *IEEE/CVF Winter Conference on Applications of Computer  
518 Vision* (2024).

519 [5] Luyu Gao, Aman Madaan, Shuyan Zhou, Uri Alon, Pengfei Liu, Yiming Yang,  
520 Jamie Callan, and Graham Neubig. 2023. PAL: Program-aided language models.  
521 *Proceedings of the 40th International Conference on Machine Learning* (2023).

522 [6] Qing Lyu, Shreya Havaldar, Adam Stein, Li Zhang, Delip Rao, Eric Wong, Mar-  
523 ianna Apidianaki, and Chris Callison-Burch. 2023. Faithful chain-of-thought

524 reasoning. *arXiv preprint arXiv:2301.13379* (2023).

525 [7] Jiayuan Mao, Chuang Gan, Pushmeet Kohli, Joshua B Tenenbaum, and Jiajun  
526 Wu. 2019. The neuro-symbolic concept learner: Interpreting scenes, words,  
527 and sentences from natural supervision. In *International Conference on Learning  
528 Representations*.

529 [8] Ramon E Moore. 1966. Interval analysis. (1966).

530 [9] Timo Schick, Jane Dwivedi-Yu, Roberta Dessi, Roberta Raileanu, Maria Lomeli,  
531 Eric Hambro, Luke Zettlemoyer, Nicola Cancedda, and Thomas Scialom. 2023.  
532 Toolformer: Language models can teach themselves to use tools. *Advances in  
533 Neural Information Processing Systems* 36 (2023).

534 [10] Hao Sha, Yao Mu, Yuxuan Jiang, Letian Chen, Chenfeng Xu, Ping Luo,  
535 Shengbo Eben Li, Masayoshi Tomizuka, Wei Zhan, and Mingyu Ding. 2023.  
536 LanguageMPC: Large language models as decision makers for autonomous driving.  
537 *arXiv preprint arXiv:2310.03026* (2023).

538 [11] Xuezhi Wang, Jason Wei, Dale Schuurmans, Quoc Le, Ed Chi, Sharan Narang,  
539 Aakanksha Chowdhery, and Denny Zhou. 2023. Self-consistency improves chain  
540 of thought reasoning in language models. *arXiv preprint arXiv:2203.11171* (2023).

541 [12] Jason Wei, Xuezhi Wang, Dale Schuurmans, Maarten Bosma, Brian Ichter, Fei  
542 Xia, Ed Chi, Quoc Le, and Denny Zhou. 2022. Chain-of-thought prompting elicits  
543 reasoning in large language models. *Advances in Neural Information Processing  
544 Systems* 35 (2022), 24824–24837.

545 [13] Zhenhua Xu, Yujia Zhang, Enze Xie, Zhen Zhao, Yong Guo, Kwan-Yee K Wong,  
546 Zhenguo Li, and Hengshuang Zhao. 2024. DriveGPT4: Interpretable end-to-end  
547 autonomous driving via large language model. *IEEE Robotics and Automation  
548 Letters* (2024).

549 [14] Shunyu Yao, Dian Yu, Jeffrey Zhao, Izhak Shafran, Thomas L Griffiths, Yuan Cao,  
550 and Karthik Narasimhan. 2023. Tree of thoughts: Deliberate problem solving  
551 with large language models. *Advances in Neural Information Processing Systems*  
552 36 (2023).

553 [15] Kexin Yi, Jiajun Wu, Chuang Gan, Antonio Torralba, Pushmeet Kohli, and  
554 Joshua B Tenenbaum. 2018. Neural-symbolic VQA: Disentangling reasoning  
555 from vision and language understanding. In *Advances in Neural Information  
556 Processing Systems*.

557

558

559

560

561

562

563

564

565

566

567

568

569

570

571

572

573

574

575

576

577

578

579

580